Silicates in Orthopaedics and Bone Tissue Engineering Materials

Xianfeng Zhou, PhD[1, 2], Nianli Zhang, PhD[4], Steven Mankoci[1], and Nita Sahai, PhD[1, 3,*]

[1]Department of Polymer Science, University of Akron, Akron, OH 44325, USA

[2]School of Polymer Science and Engineering, Qingdao University of Science and Technology, Qingdao, Shandong Province, 266042, China

[3]Integrated Bioscience Program and Department of Geology, University of Akron, OH 44325, USA

[4]Department of Biologic and Materials Sciences, University of Michigan, Ann Arbor, MI 48109, USA

[*]Corresponding author: N.S.

E-mail: sahai@uakron.edu

Fax: +1-330-972-7001

Phone: +1-330-972-5795

Acknowledgments: Financial support was provided by NSF DMR (0906817), start-up funds from the University of Akron and the Ohio Research Scholar Program to Dr. Nita Sahai, PI.

ABSTRACT

Following the success of silicate-based glasses as bioactive materials, silicates are believed to play important roles in promoting bone formation and have therefore been considered to provide a hydroxyapatite surface layer capable of binding to bone as well as potentially being a pro-osteoinductive factor. Natural silicate minerals and silicate-substituted hydroxyapatites are also being actively investigated as orthopaedic bone and dental biomaterials for application in tissue engineering. However, the mechanisms for the proposed roles of silicate in these materials have not been fully understood and are controversial. Here, we review the potential roles of silicate for bone tissue engineering applications and recent breakthroughs in identifying the cellular-level molecular mechanisms for the osteoinductivity of silica. The goal of this article is to inspire new ideas for the rational design of third-generation cell-and gene-affecting biomaterials.

KEYWORDS: silicate (silica, silicon); bioactive materials; osteoblast; osteoclast; mechanism.

1. Introduction

The importance of replacing or regenerating bone becomes clear in the cases of diseases such as osteogenesis imperfecta, Paget's disease, and osteoporosis in which normal bone development or turnover are impaired, and in situations where bone is surgically removed because of severe trauma or infection [1]. Replacement of damaged, diseased or aged bone tissue has become routine as a result of the development of reliable and affordable biomaterials and perfection of surgical procedures for implantation of prostheses and subsequent rehabilitation of patients [2]. The treatments involving bone repair and replacement have improved and saved countless lives [3]. Since the development of the concept of tissue engineering, the emphasis on developing novel materials has shifted from bone tissue replacement to tissue regeneration [4].

Bone tissue engineering requires bioactive and osteoinductive materials that mimic some of the features of native bone tissue, present a physiochemical biomimetic environment, and actively promote desirable responses. To address these requirements, a variety of materials have been investigated including metals, glasses, ceramics, polymers and composites of these materials. Ceramics and glasses of specific compositions are considered to be bioactive as they can bond to bone and enhance bone tissue formation. These formulations of ceramics and glasses include not only the chemical constituents (calcium and phosphate) of natural bone mineral, but also silicate, which normally occurs at trace levels in bone [5, 6]. The choice of calcium and phosphate is not surprising as these ions constitute the mineral phase of bone [7], but it is hard to understand why and how silicate works. In this paper, we first provide a brief history of how silicate entered the field of orthopaedic biomaterials and tissue engineering materials. Different types of silicate-based biomaterials, including glasses and ceramics are reviewed, and the roles of silicate in these materials are highlighted along with recent contradictory reports in the

literatures. Finally several mechanisms that can potentially explain the biological roles of silicate are presented.

2. Why silicate?

Silicon (Si) is the eighth-most common element in the universe by mass, and the second-most abundant element in the earth's crust (about 28% as various forms of silica or silicate) after oxygen [8]. Si is also found in all living organisms [5]. It has been proposed to play an important biological role in humans [5] and play an essential role in organisms such as diatoms that use SiO_2 to produce their exoskeleton [9-12]. Si is present at a level of ~ 1 ppm in the serum, 2-10 ppm in the liver, kidney, lungs and muscle, 100 ppm in bone and 200-600 ppm in cartilage and other connective tissue [13]. The earliest study of Si in bone dates back to the early 1970s. Using electron probe microanalysis, Carlisle observed that Si levels were highest (0.5 wt%) during the earliest stages of bone calcification when Ca/P ratios are low (Ca/P = 0.7) compared to the ratio (Ca/P = 1.67) in stoichiometric hydroxyapatite (HAP). Subsequently, Si levels were observed to fall below the detection limit as mineralization proceeded, and the Ca/P of bone increased towards that of ideal stoichiometric HAP ($Ca_{10}(PO_4)_6(OH)_4$) [14]. Thus, Si was shown to be localized at active calcification sites in the bones of young mice and rats. Additionally, Si-deprivation experiments were performed in chicks [15] that were fed a diet consisting of casein and corn with a very low silicate content of 2 mg/g or fed the same diet supplemented with 100 mg/g Si as sodium metasilicate. After 4 weeks, the average mass of Si-deprived chicks was 76 g, compared to the mass of 116 g for Si-supplemented chicks. Skull deformities (shorter skull and distortion around the eye sockets), shorter, thinner, and more flexible limb bones that were easily fractured as well as the absence of a wattle and comb were reported in the Si-deprived chicks [15]. Lower levels of collagen were also observed in the cartilage of Si-deficient chicks, but no

difference in the level of non-collagenous proteins [16, 17]. Carlisle *et al*. demonstrated that Si was required for normal bone growth and development in higher animals (Fig. 1). In a similar study by Schwartz and Milne in rats, hair loss, seborrhoea, loss of muscle tone, disturbances in enamel development and impairment of incisor pigmentation were observed [18]. Taken together, these findings indicated potentially important roles of Si in the formation of bone and other connective tissues such as cartilage. Therefore, Si may be categorized as an essential trace element for metabolic processes associated with the development of bone and connective tissues, and the localization of Si is at the growing front of bone.

Figure 1

A recent study using dietary Si supplementation in ovariectomized mice showed that trabecular bone volume decreased by 48% in untreated animals compared to the groups which received either aqueous silicate or estradiol, an inhibitor of the resorption activity of osteoclasts [19]. Si deficiency in ovariectomized animals also lead to a decrease in the concentration of plasma osteopontin, an important factor in bone remodeling, especially in anchoring osteoclasts to the mineral matrix of bone [20]. Furthermore, differences in dietary Si intake were positively and significantly linked to bone mineral density (BMD) at all hip measurement sites in men and premenopausal women with BMD differences as large as 10% between the highest (> 40 mg Si/day) and lowest levels (< 14 mg Si/day) of Si intake [21]. Si played a role in the remodeling process of bone [19, 20] and may inhibit the physiological resorption process.

In summary, Si appears to be required for the formation of bone and is associated with both the inorganic and the organic phases of bone. Hence, Si has been incorporated in the design of many orthopaedic implant materials.

3. Silicate in biomaterials

3.1 Silicate in bioactive glasses

The positive effect of Si on bone metabolism has raised the interest of research groups working on bone graft substitutes. In the early 1970s, Hench and his co-workers discovered that specific melt-derived four-component glasses composed of SiO_2, CaO, Na_2O and P_2O_5 could bond with bone after implantation *in vivo* without the need for a cement at the time of surgery [22-26]. When immersed in biological fluids, a layer of HAP or hydroxyl carbonated apatite (HCA) similar to the mineral phase of bone, was deposited on the glass surface. Therefore, these specific glasses were termed bioactive because they promoted a positive response from the tissue; more specifically, they are osteoconductive. The bonding rate to existing bone tissue was specific to the bioactive glass composition [27]. In particular, the most rapid rates of bonding were obtained for bioactive glasses with SiO_2 contents of 45-52 wt%, which bonded to both soft and hard connective tissue within 5-10 days. Bioactive glasses containing 55-60 wt% SiO_2 required a longer time to bond with bone but did not bond to soft tissue [28]. Glass compositions with more than 60 wt% SiO_2 were biologically inert because they bonded neither to bone nor to soft tissues and, eventually, elicited the formation of a non-adherent fibrous interfacial capsule (Fig. 2) [29].

Figure 2

The index of bioactivity (I_b) is defined as the inverse of the time required for more than 50% of the bone-material interface to be bonded ($I_b = 100/t_{0.5bb}$). In the SiO_2-CaO-Na_2O-P_2O_5 system, glass compositions from 40-52 wt% SiO_2 have I_b values varying from 12.5 to 10. The most bioactive composition (45 wt% SiO_2, 24.5 wt% CaO, 24.5 wt% Na_2O and 6 wt% P_2O_5) was named "Bioglass®". This was the first bioactive material, discovered in 1969 [30], and has found

many applications in the orthopaedic and dental fields. Even today it is considered to be one of the most successful materials to regenerate bone [22].

Clark and Hench [31] first proposed a detailed sequence of reactions occurring *in vitro* at the surface of silicate-based bioactive glasses immersed in simulated body fluid (SBF): (i) rapid exchange of Na^+ and Ca^{2+} in the glass with H^+ in solution; (ii) release of soluble silicate as $Si(OH)_4$ by hydrolysis of Si-O-Si bridges in the glass with the formation of surface silanol groups; (iii) condensation and repolymerization of surface silanols with soluble silicate to form an amorphous SiO_2-rich surface layer; (iv) migration of Ca^{2+} and PO_4^{3-} to the surface through the silica-rich layer and formation of a calcium phosphate (CaP) rich layer on the glass surface; (v) incorporation of OH^- and CO_3^{2-} from the solution and subsequent crystallization of the Ca-P layer to form HCA (Fig. 3, [32]). After these physical-chemical reactions occur, biological moieties can interact with the glass surface. Collagen molecules are incorporated in the HCA layer, and then cells begin to respond, leading ultimately to bone growth. The bonding mechanism was proven via microscopy, which showed the interface between bone and bioactive glass in a 4-week rat tibial implant [31].

Figure 3

The behavior of glasses of different compositional ranges was explained on the basis of the rate of dissolution compared to the rates of cell responses such as attachment, proliferation and differentiation. Thus, it was noted that Fig. 2 represents kinetic boundaries and is not a phase diagram. Only glasses that dissolve rapidly bond to soft tissue (Region E in Fig. 2) and glasses with more than 52 wt % SiO_2 bond to bone but not to soft tissue. For glasses that dissolve too slowly, the concentrations of the released ionic products are too low to promote cell proliferation and differentiation.

The authors also defined two classes of bioactivity based on the glass compositional range and biological response elicited. Class A bioactive glasses dissolve rapidly and induce both extracellular and intracellular responses (i.e., are both osteoconductive and osteoinductive), whereas class B bioactive materials dissolve more slowly and elicit only extracellular responses (i.e., are only osteoconductive). Note that these "A" and "B" classes are not to be confused with regions A and B in Fig. 2.

3.2 Silicate in calcium phosphate bioceramics

Synthetic stoichiometric HAP has been utilized extensively as a skeletal replacement material. However, synthetic HAP exhibits limited ability to form an osteoconductive bond with existing bone *in vivo* in a rabbit model; the response may take several days [33] when compared to bioactive glasses in which the reactions occur in just a few minutes [34]. Moreover, stoichiometric HAP is relatively insoluble and does not degrade significantly, which can be a limiting factor in creating space for new bone tissue formation [35]. Additionally, the mineral found in bone is not a stoichiometric compound, but exhibits variable deficiencies in Ca, P and OH [36]. Various substitutions exist in bone mineral, in particularly, carbonate anion is found at up to 8 wt%, as well as elements such as Na, Mg, K, Sr, Zn, Ba, Cu, Al, Fe, F, Cl, and Si that can occur at trace (< 1 wt%) levels [37]. These substitutions in the apatite structure play important roles in the biological activity of bone mineral by influencing the solubility, surface chemistry, crystal size, and morphology of the bone mineral. Inspired by the positive effects of silicate on bone metabolism, some research groups have made efforts to develop silicate-containing CaP as bone graft substitutes, such as silicate-substituted HAP [38] and silicate-substituted tricalcium phosphate ($Ca_3(PO_4)_2$, TCP) [39].

3.2.1 Silicate-substituted HAP (Si-HAP)

In Si-HAP, silicate anions (SiO_4^{4-}) substitute phosphate anions (PO_4^{3-}) directly in the apatite crystal lattice (Fig. 4, [40, 41]). The amount of silicate is incorporated with only a limited values ranging from 0.1 to 1.6 wt% [42]. However, small amounts (0.5 and 1 wt%) are apparently sufficient to yield significant improvements in the formation of a new layer of hydroxyapatite and in cell proliferation *in vitro* compared to pure HAP [43]. For example, when pure HAP and Si-HAP were immersed in SBF for five weeks, the surface of pure HAP remained almost unchanged. In contrast, Si-HAP developed a new surface HAP phase with acicular and plate-like morphology, similar to that of new apatite phases grown on bioactive glasses [43]. Additionally, *in vitro* cell culture tests showed that Si-HAP is non-cytotoxic to human osteosarcoma cells (HOC) [40]. Cell proliferation was determined by measuring the mitochondrial activity via MTT (3-(4,5-dimethylthiazol-2-yl)-2,5-diphenyltetrazolium bromide) assay. The higher the silicate content (up to 1.6 wt%), the higher was the cell proliferation from the first day to one week of culture. These findings are also in agreement with the observed effect of zeolites in promoting osteoblast proliferation and the expression of transforming growth factor beta (TGF-β) mRNA in human osteoblast-like cells [44]. Moreover, *in vivo* studies indicated that the early bioactivity of HAP was significantly improved with the incorporation of silicate ions into the HAP structure. In a comparative study, new bone formation was also observed directly on the surfaces and in the space between both HAP and Si-HAP (0.8 wt%) granular implants in a white rabbit model [45]. The percentage of bone ingrowth for Si-HAP (37.5 ± 5.9 %) was significantly greater than that for pure HAP (22.0 ± 6.5 %). Additionally, the percentage of bone/implant coverage was significantly greater for Si-HAP (59.8 ± 7.3 %) compared to HAP (47.1 ± 3.6 %) [45].

Figure 4

Bone remodeling around the implant also occurred faster when silicate was incorporated into HAP. This may be due to the higher dissolution rates of the Si-HAP implants compared to pure HAP [46]. The substitution of SiO_4^{4-} for PO_4^{3-} in the HAP lattice yields tetrahedral distortion and disorder at the hydroxyl site, which could decrease the stability of the apatite structure and also decrease the grain size [42]. Compared to pure HAP, the smaller grain size and the formation of a less ordered grain boundary in the Si-HAP increases the solubility and affects the timing of deposition of the new HAP layer at the bone-implant interface [46-49]. Furthermore, Si has been confirmed by X-ray photoelectron spectroscopy (XPS) to exist as an isolated tetrahedral silicate, SiO_4^{4-} group, rather than in a polymeric SiO_2 form [50]. The presence of SiO_4^{4-} is important, because the SiO_4^{4-} group is preferentially substituted by PO_4^{3-}. The faster *in vitro* apatite formation would be a consequence of this fact. Therefore, the mechanism of the silicate action should be considered as a sum of different factors at different levels.

3.2.2 Silicate-substituted TCP (Si-TCP)

TCP occurs as alpha (α-TCP) and beta (β-TCP) crystal polymorphs, and the α-TCP phase is formed only at temperatures higher than 1,200 ºC. Both phases can be used as orthopaedic biomaterials alone or in conjunction with a biodegradable polymer, such as polyglycolic acid [51]. Silicate substituted α-TCP (Si-α-TCP) exhibited enhanced bone apposition, bone in-growth and cell mediated degradation compared to stoichiometric counterparts [52]. The bioactivity of Si-α-TCP increased with an increasing silicate ion substitution [53]. In particular, the surface of 2.23 wt% Si-α-TCP was partially covered by HAP after one week, and complete coverage was attained in the same time on the surface of 8.1 wt% Si-α-TCP. The results were interpreted to indicate that porous microstructure of high-concentration Si-TCP helped the dissolution of surface ions and the leaching process. Thus, SBF reached super-saturation with respect to HAP

in a short time and accelerated the deposition of HAP [53]. In contrast, Camire *et al*. found the thickest HAP layer (the greatest bioactivity) was formed on the surface of 1 wt% Si-TCP, compared to 3, 5 wt% Si-TCP [54]. The result was also supported by *in vivo* study. Comparing the cement containing 1% silicate-doped α-TCP with pure α-TCP indicated that silicate presence in the matrix enhanced mesenchymal cell differentiation and osteoblast activity in rabbits [54]. In another long term *in vivo* study, the performance of Si-TCP implant was investigated in sheep. The authors found that only 10–20% of the scaffold remained after 1 year. The scaffolds were completely resorbed after 2 years and were replaced by newly-formed highly-mineralized lamellar bone tissue (Fig. 5) [55]. None of the implanted bioceramics were reported to produce any adverse effects, such as inflammation.

Figure 5

Currently, two different silicate-substituted CaPs are used in clinical bone substitute applications. Single-phase Si-HAP materials are manufactured commercially by Apatech Ltd. under the trade name Actifuse™. Si-stabilized CaPs composed primarily of Si-α-TCP are manufactured commercially by Millenium Biologix Corporation under the trade name Skelite™. Actifuse™ and Skelite™ are both prepared in microporous scaffold and/or granules intended for filling bone defects in non-load-bearing applications.

3.3 Bioactive silicate ceramics

It was long believed that in order to be bioactive, glasses and glass-ceramics must contain both CaO and P_2O_5, which are the main components of the HAP. However, Ohura *et al*. [56] observed that CaO-SiO_2 glasses free of P_2O_5 as well as those containing very small amounts of P_2O_5, formed a surface HAP layer, when immersed in SBF and interestingly, CaO-P_2O_5 glasses free of SiO_2 did not form a HAP layer. This seemed to indicate that bioactive materials can be obtained

with compositions based on the CaO-SiO_2 system rather than on CaO-P_2O_5. Taking into account these observations, some silicate ceramics such as $CaSiO_3$ have been tested for their potential bioactivity.

3.3.1 $CaSiO_3$

In the 1990s De Aza and co-workers demonstrated the bioactivity of β-$CaSiO_3$ (pseudowollastonite, a high temperature polymorph) and α-$CaSiO_3$ (wollastonite, a low temperature polymorph). Both $CaSiO_3$ phases can form a surface HAP layer after exposure to SBF *in vitro* and bond to living bone *in viv*o [57-63]. Subsequently, numerous other studies demonstrated that the two $CaSiO_3$ phases are promising candidate materials for bone replacement. The two polymorphs of $CaSiO_3$ have identical chemical composition and stoichiometry but different crystal structures, which can affect their bioactive properties. In β-$CaSiO_3$, three silicate tetrahedra are covalently bonded via corner-sharing oxygens to form "silicate 3-rings", whereas α-$CaSiO_3$ is made up of corner-sharing silicate tetrahedral covalently linked to form silicate chains (Fig. 6). The silicate "3-rings" structure found in β-$CaSiO_3$ is similar to the "3-rings" defect sites in bioactive glasses [64, 65]. The negative charge associated with the silicate rings and chains respectively, is electrostatically balanced by Ca^{2+} ions. The high strain associated with the Si-O-Si bond angles in the "3-rings" of β-$CaSiO_3$ makes these bonds much more susceptible to hydrolysis than the more stable Si-O-Si bonds in the α-$CaSiO_3$ chains. This results in the greater solubility and dissolution rate of β-$CaSiO_3$ compared to α-$CaSiO_3$ [66, 67]. In our group, we studied the kinetics of dissolution of the β-$CaSiO_3$ and α-$CaSiO_3$ in cell culture medium [68]. Soluble silicate concentrations peaked at higher levels and earlier time points for β-$CaSiO_3$ than for α-$CaSiO_3$, consistent with the higher solubility and

dissolution rate of the three-ring structure versus the chain silicate structure, which may be the reason that β-$CaSiO_3$ is more bioactive than α-$CaSiO_3$.

Figure 6

The cytotoxicity of β-$CaSiO_3$ [69], and the suitability of the material as a substratum for cell attachment and its ability to affect osteoblast behavior at a distance from the material surface [70] have been evaluated. These experiments demonstrated that β-$CaSiO_3$ were not significantly cytotoxic. In our *in vitro* experiments, we found that a high concentration of silicate (> 120 ppm) released from β-$CaSiO_3$ is initially cytotoxic towards human mesenchymal stem cells (hMSCs), but cell proliferation increased once lower steady-state soluble silicate concentrations (~ 80 ppm) were achieved [67, 68].

In vivo experiments have also been conducted in which small cylinders of β-$CaSiO_3$ were implanted into rat tibias [71]. Histological observations showed the new bone was growing in direct contact with the β-$CaSiO_3$ implants after only 3 weeks. After twelve weeks implantation the bone in contact with the surface of the β-$CaSiO_3$ appeared to be progressively replaced by bone with lamellar structure similar to native bone. At twelve weeks of implantation, new bone was still growing at the interface.

3.3.2 Silicate ceramic composites

Despite the success of various silicate-based materials for bone replacement, one of the most important outstanding problems is implant osteointegration (ingrowth of new bone into the implants). When bioactive materials are implanted *in vivo*, the interactions between the bone tissue and these materials usually take place only on their surfaces, while the bulk of the material remains unchanged. In multiple cases, this has caused a harmful shear stress at the bone-implant interface [71, 72]. To improve the osteointegration, the scaffold must have a high degree of

porosity [73]. However, ceramics and bioactive glasses are formed as porous scaffolds, so the macroscopic mechanical properties are inadequate for loading-bearing applications because of the inherent brittleness of ceramics. This drawback seriously limits the clinical relevance of ceramics as synthetic bone scaffolds [29, 74].

A wide variety of ceramic-ceramic, ceramic-polymer and glass-ceramic composites have been developed to address this concern. Bioeutectic® is one such composite, which is capable of developing a porous HAP-like structure *in situ* when they are implanted into a living body. Bioeutectic® consists of bioactive β-$CaSiO_3$ and resorbable α-TCP, and presents a high reactivity in SBF [63]. When the β-$CaSiO_3$ phase came in contact with the SBF, it reacted via an ion exchange of two H^+ from the SBF for one Ca^{2+} from β-$CaSiO_3$ (Fig. 7a). This exchange resulted in the formation of a surface amorphous silica layer and also caused the pH at the material/SBF interface to increase to 8.9. Immediately following this reaction, the TCP lamellae started to react with the Ca^{2+} and OH^- ions present in the confined channels [63]. As a result, a pseudomorphic transformation of α-TCP into apatite occurred according to the reaction:

$$3Ca_3(PO_4)_2 + Ca^{2+} + 2OH^- \rightarrow Ca_{10}(PO_4)_6(OH)_2$$

The silicate and excess Ca^{2+}, which were not involved in the reaction, migrated through the SBF solution away from the interface and into the solution. However, a large increase was not detected for Ca^{2+} concentration in solution. So most of the Ca^{2+} must have reacted with the phosphate of the SBF, leading to the precipitation of HAP on the surface of the material according to the reaction:

$$6HPO_4^{2-} + 10Ca^{2+} + 8OH^- \rightarrow Ca_{10}(PO_4)_6(OH)_2 + 6H_2O$$

The overall reaction resulted in a large increase in Si concentration in the SBF, a small increase in Ca, and a decrease in P, as detected by inductively coupled plasma-atomic emission spectroscopy (Fig. 7b).

Figure 7

For *in vivo* studies, Bioeutectic® implants were inserted into the critical size defects of rabbits' tibiae. The results showed a new fully mineralized bone growing in direct contact with the implants. The osteoblasts migrated towards the interface and colonized the surface at the contact areas with the bone [75]. Thus, Bioeutectic® ceramic could be satisfactorily used for repair or replacement of bone.

3.4 Bioactive porous silica

In 1992, Li *et al*. reported the formation of HAP on silica gels when the gels were in contact with SBF, but not on dense silica glasses or quartz [76]. The mesoporous silica, having pore sizes in the range of 2-90 nm and inner surface silanol, have been shown as bioactive materials for tissue regeneration [77]. Bioactivity studies have been carried out on porous silica materials, such as SBA-15 (Santa Barbara Amorphous type material), MCM-48 (Mobil Crystalline Materials) and MCM-41 [77, 78] (Fig. 8). SBA-15 developed a HAP layer after 30 days immersion in SBF, while 60 days were required for MCM-48, a HAP layer did not form at all on MCM-41. The different behaviors of the three mesoporous materials were explained on the basis of the compositional, textural and structural properties. As already mentioned above, surface silanol groups may act as nucleation sites for HAP layer. The silanol group concentration seems to be an important factor. The Si-OH concentration per unit surface area was determined by thermo-gravimetric analyses (TGA) and N_2 adsorption measurements. MCM-41 showed a rather low concentration of silanol groups (*ca*. 2.2 mmol SiOH m^{-2}) compared to SBA-15 (*ca.* 12.7

mmol SiOH m^{-2}) and MCM-48 (*ca*. 12.9 mmol SiOH m^{-2}). This could be one reason to explain the absence of bioactivity in MCM-41. The textural and structural properties of the mesoporous silica were also taken into account. Usually, bigger and more accessible pores will favor ion diffusion and faster HAP nucleation. SBA-15 showed the largest pore size (8.8 nm) compared with MCM-48 (3.6 nm) and MCM-41 (3.6 nm), which may have been responsible for the faster HAP nucleation kinetics on SBA-15 compared to MCM-48 and MCM-41.

Figure 8

3.5 Bioactive porous silicon

Microporous Si itself has been shown to be bioactive [79]. Similar to bioactive ceramics, hydrated poly-Si layers with suitable microstructure induced HAP deposits. However, the semiconductor Si has never been considered a promising biomaterial compared to numerous ceramics and polymers [80] because it has poor hemocompatibility [81]. However, with simple wet-etching (nano-etching) [79] or electrochemical etching techniques in HF-based electrolytes [82], Si wafers can be rendered highly bioactive. *In vitro* studies in SBF showed that microporous Si film could induce HAP growth on top of the porous Si and even on neighboring areas of bulk Si [79]. Unlike polished Si wafer, which do not degrade in cell medium, porous Si could degrade. The experiments showed that freshly etched mesoscale Si (*ca*. 50 nm, MesPSi) degraded faster than macroscale Si (*ca*. 1 μm, MacPSi) in cell culture medium [82]. Furthermore, MacPSi performed better than MesPSi and NanPSi (< 15 nm, nanoscale porous Si) in supporting osteoblast growth, differentiation and sustaining their function. In summary, PSi, especially MacPSi, which has a large surface-to-volume ratio and flexible surface chemistry, make it appealing for microscale devices with both drug-delivery and scaffolding functions. These results proved that, if hydrated, Si itself could become an important tissue-compatible

biomaterial, and could potentially have widespread applications in biomedicine and tissue engineering. However, note that the hydration results in the formation of a surface layer of silica or at least silanol surface sites. So the apparent bioactivity of Si is most likely related to silica.

4. The controversial roles of silicate

After almost 50 years of development of silicate-based biomaterials as orthopaedic implants, the scientific community widely accepts the statements that silicate-substituted materials have better biological properties in bone tissue engineering compared to their silicate-free counterparts. Based on the reports and discussion above, a passive mechanism has been suggested that the presence of Si in the materials cause chemical, physical, or topographical changes at the surface that eventually lead to a change of the biological response [83].

Yet, the role of silicate may go beyond the simple osteoconductivity (the ability to form HAP surface layer that bonds to bone) of silicate materials and may include influences on cell activity (cell proliferation and differentiation). The inorganic dissolution products ($Si(OH)_4$, Ca^{2+}, PO_4^{3-}, *etc*.) released from bioactive glasses have been proven to influence and control the cell cycle of osteogenic precursor cells and, ultimately, control cell differentiation [84, 85] at a specific concentration range of silicate and Ca^{2+} [2]. Xynos *et al.* discovered that critical concentrations of these dissolution products could activate or up-regulate seven families of genes in osteogenic cells (Table 1). These genes encode transcription of numerous proteins that control the cell cycle, proliferation and, ultimately, the differentiation of cells towards the mature osteoblastic phenotype [2, 85-87]. Similarly, the dissolution products from Si-TCP were reported to have dose-dependent effects on osteoblast proliferation and differentiation, osteoclast formation and the resorption process, and also influence the formation of the extracellular matrix [52, 88]. Therefore, an "active role" was claimed that silicate can affect bone cell metabolism [5].

Table 1

However, some groups have challenged these concepts. In one study, Si-HAP was demonstrated not to dissolve *in vitro* during more than two weeks in a solution containing 10 times less Ca^{2+} and 100 times less phosphate ions than in serum [89]. An *in vivo* study showed material resorption in a weight-bearing long bone sheep model [55], but silicate release concentrations or the silicate levels required for therapeutic effects were not determined in any of these studies. Therefore, in a critical review [83], it was questioned whether silicate could enhance the dissolution of CaP and whether silicate in Si-CaPs can be released *in vivo* and attain a therapeutic level. Furthermore, the roles of silicate to activate or up-regulate genes in cells had also been doubted because most of the arguments to support the active roles of silicate were based on the dissolution products of bioactive glasses/ceramics, which result in a multicomponent solution rather than only dissolved silicate. Moreover, some recent studies investigating the essentiality of silicate in growing animals [90-94] have failed to reproduce the dramatic results reported by Carlisle [15] and by Schwarz and Milne [18]. Although differences in experimental conditions, such as duration of the experiment, age, gender and species of the animals, Si source and route of administration, as well as overall nutritional compositions of the basal diet may all have contributed to the inter-experimental variance [95], the role of silicate in natural bone mineralization might be over-evaluated.

To address these concerns, Reffitt *et al*. [96] showed that 10 μM and 20 μM orthosilicic acid (H_4SiO_4) addition to MG63 osteosarcoma cells increased collagen type I (Col I) levels 1.75-fold. Increasing concentrations of H_4SiO_4 (0-50 μM) in primary human osteoblast cells also resulted in increased Col I production by increasing mRNA transcription or mRNA stabilization [97, 98], which suggested a structural role (stabilization of collagen) or a metabolic role (a co-factor for

prolyl hydroxylase) for silicate [95]. H_4SiO_4 also increased the gene expression of osteocalcin and alkaline phosphatase, which are indicators of osteogenic differentiation and mineralization [99, 100]. Recently, soluble silicate has been reported to enhance the human osteoblast metabolic activity, proliferation, and differentiation [101] and inhibit osteoclast formation and bone resorption *in vitro* [102]. However, none of these studies attempted to determine the mechanistic roles of silicate.

More recently, silica (SiO_2) nanoparticles [103] and nanoplatelets [104] were shown to mediate potent stimulatory effects on osteoblast differentiation. It was shown that a specific size of silica nanoparticle (50 nm in diameter) can antagonize the activation of nuclear factor kappa-light-chain-enhancer of activated B cells (NF-κB), a signal transduction pathway that can inhibit osteoblastic bone formation but promote osteoclastic bone resorption [103]. These silica nanoparticles could enter the cells through a caveolae-mediated endocytosis, which triggers the stimulation of the mitogen activated protein kinase (MAPK) ERK1/2 (p44/p42) pathway and stimulates autophagosome assembly [105]. Although still not completely understood, this process (Fig. 9) is stimulatory to osteoblast differentiation and mineralization. However, as the authors recognized, subtle changes in charge, shape, size, and/or surface chemistry of these silica particles may lead to very different physicochemical responses of cells [103]. For example, hexagonal silica nanoparticles with size about 100 nm did not show any bioactive effect *in vitro* [106]. Therefore, it is possible that not silicate but, the nano-sized solid particles could be responsible for these positive biological outcomes. Biosilica, the inorganic scaffold that forms the siliceous skeleton in sponges, was reported to induce the expression of osteoprotegerin (OPG). By using a Boyden chamber co-culture system, some research groups concluded that the inhibition of osteoclastogenesis of RAW264.7 pre-osteoclasts was due to the increased level of

OPG released by osteoblasts after exposure to silicate. The receptor activator of nuclear factor kappa-B ligand (RANKL) may be bound by OPG, which can abolish RANKL function to inhibit osteoclast differentiation (Fig. 10, [107]).

In our group, we have investigated the effects of soluble silicic acid on osteogenic differentiation of human mesenchymal stem cells (hMSCs) and osteoclastic differentiation of mouse hematopoietic stem cells (mHSCs) [108]. At the physiological pH and concentrations below 2 mM, Si exists predominantly as monomeric $Si(OH)_4$. This $Si(OH)_4$ is uncharged at neutral pH, but has the tendency to polymerize to polysilicate at Si concentration above ~ 2 - 3 mM [109]. Below this concentration, our studies showed that soluble $Si(OH)_4$ stimulates the proliferation of hMSCs and mHSCs in normal growth medium. More interestingly, we found the $Si(OH)_4$ regulated bone formation and bone resorption by promoting osteoblastic gene program while repressing osteoclast differentiation [108]. To elucidate the possible molecular mechanisms, differential microRNA microarray analyses were applied. Results showed that microRNA-146a (miR-146a) was significantly up-regulated in bone cells treated with $Si(OH)_4$. Inhibition of miR-146a function by anti-miR-146a suppressed osteogenic differentiation of pre-osteoblasts, whereas $Si(OH)_4$ treatment counteracted this inhibition and promoted osteoblast-specific gene transcription and protein expression. Furthermore, both miRNA-146a and $Si(OH)_4$ were shown to decrease TNFα (or RANKL)-induced activation of NF-κB in bone cells. Therefore, our studies established a mechanism for silicate to promote osteogenesis and suppress osteoclast formation by antagonizing NF-κB signaling via miR-146a (Figure 11).

The above discussion suggests an active role for dissolved silicate and silica nanoparticles (50 nm size) in affecting cell behavior *in vitro* by specific molecular biology pathways These ground-breaking studies are showing that silicate not only promotes osteogenic differentiation of

hMSCs but also suppresses osteoclastic differentiation of mHSCs and osteoclast bone resorption activity [102-105]. Thus, silicate-based biomaterials that release soluble silicate can be considered not simply as bone graft substitutes but are, effectively, drug delivery systems in which soluble silicate acts like a drug. For example, $Si(OH)_4$ could be used as a nutritional supplement to treat osteoporosis, a disease which results due to an imbalance between bone formation and resorption, which is common in women after menopause and older men [21, 95].

Figure 9

Figure 10

Figure 11

5. Summary

The effect of silicate on bone formation has long been recognized and debated in the literature. Controversy arose in resolving whether an effect exists and, if so, is it by a passive or active mechanism because of differences in experimental conditions, cell types and animal models, presence of other dissolved ions along with silicate, the effects of truly dissolved silicate versus the effect of solid biomaterial surfaces, dose-effects of dissolved silicate released from various silica-containing biomateirals etc. The results of more carefully-designed recent studies are adding to a growing body of evidence for an active role of dissolved silicate and solid silica nanoparticles of specific size.

Acknowledgements: N.S. gratefully acknowledges financial support by NSF DMR 0906817, the University of Akron "Start-Up" Funds and the State of Ohio for the Ohio Research Scholar-Biomaterials Funds.

Reference

[1] Porter JR, Ruckh TT, Popat KC. Bone tissue engineering: a review in bone biomimetics and drug delivery strategies. Biotechnol Prog 2009;25:1539-60.

[2] Hench LL. Genetic design of bioactive glass. J Eur Ceram Soc 2009;29:1257-65.

[3] Langer R, Vacanti J. Tissue engineering. Science 1993;260:920-6.

[4] Hench LL, Polak JM. Third-Generation Biomedical Materials. Science 2002;295:1014-7.

[5] Jugdaohsingh R. Silicon and bone health. J Nutr Health Aging 2007;11:99-110.

[6] Cerruti M, Sahai N. Silicate Biomaterials for Orthopaedic and Dental Implants. Rev Mineral Geochem 2006;64:283-313.

[7] Newman WF, Newman MW. The Chemical Dynamics of Bone Mineral. Am J Med Sci 1959;238:789.

[8] Yaroshevsky A. Abundances of chemical elements in the Earth's crust. Geochem Int 2006;44:48-55.

[9] Sahai N, Tossell JA. Formation energies and NMR chemical shifts calculated for putative serine-silicate complexes in silica biomineralization. Geochim Cosmochim Acta 2001;65:2043-53.

[10] Sahai N, Tossell JA. 29Si NMR Shifts and Relative Stabilities Calculated for Hypercoordinated Silicon−Polyalcohol Complexes: Role in Sol−Gel and Biogenic Silica Synthesis. Inorg Chem 2002;41:748-56.

[11] Sahai N. Silicon-Organic Interactions in the Environment and in Organisms. Geochemical and Hydrological Reactivity of Heavy Metals in Soils: CRC Press; 2003.

[12] Sahai N. Calculation of 29Si NMR shifts of silicate complexes with carbohydrates, amino acids, and muhicarboxylic acids: potential role in biological silica utilization. Geochim Cosmochim Acta 2004;68:227-37.

[13] Schwarz K. A Bound Form of Silicon in Glycosaminoglycans and Polyuronides. Proc Natl Acad Sci U S A 1973;70:1608-12.

[14] Carlisle EM. Silicon: a possible factor in bone calcification. Science 1970;167:279-80.

[15] Carlisle EM. Silicon: an essential element for the chick. Science 1972;178:619-21.

[16] Carlisle EM. The nutritional essentiality of silicon. Nutr Rev 1982;40:193-8.

[17] Carlisle EM. Silicon as an essential trace element in animal nutrition. Ciba Found Symp 1986;121:123-39.

[18] Schwarz K, Milne DB. Growth-promoting effects of silicon in rats. Nature 1972;239:333-4.

[19] Hott M, de Pollak C, Modrowski D, Marie PJ. Short-term effects of organic silicon on trabecular bone in mature ovariectomized rats. Calcif Tissue Int 1993;53:174-9.

[20] Nielsen FH, Poellot R. Dietary silicon affects bone turnover differently in ovariectomized and sham-operated growing rats. J Trace Elem Exp Med 2004;17:137-49.

[21] Jugdaohsingh R, Tucker KL, Qiao N, Cupples LA, Kiel DP, Powell JJ. Dietary silicon intake is positively associated with bone mineral density in men and premenopausal women of the Framingham Offspring cohort. J Bone Miner Res 2004;19:297-307.

[22] Hench LL, Splinter RJ, Allen WC, Greenlee TK. Bonding mechanisms at the interface of ceramic prosthetic materials. J Biomed Mater Res 1971;5:117-41.

[23] Hench LL. The story of Bioglass®. J Mater Sci: Mater Med 2006;17:967-78.

[24] Hench LL. Bioceramics. J Am Ceram Soc 1998;81:1705-28.

[25] Vallet-Regi M, Salinas AJ, Roman J, Gil M. Effect of magnesium content on the in vitro bioactivity of CaO–MgO–SiO2-P2O5 sol-gel glasses.pdf. J Mater Chem 1999;9:4.

[26] Jones JR, Gentleman E, Polak J. Bioactive Glass Scaffolds for Bone Regeneration. Elements 2007;3:393-9.

[27] Hench LL. Bioactive Ceramics. Ann N Y Acad Sci 1988;523:54-71.

[28] Wilson J, Pigott GH, Schoen FJ, Hench LL. Toxicology and biocompatibility of bioglasses. J Biomed Mater Res 1981;15:805-17.

[29] Hench LL. Bioceramics: From Concept to Clinic. J Am Ceram Soc 1991;74:1487-510.

[30] Hench L. Apparatus for producing strands or granules from liquid material. 1969.

[31] Clark AE, Hench LL, Paschall HA. The influence of surface chemistry on implant interface histology: A theoretical basis for implant materials selection. J Biomed Mater Res 1976;10:161-74.

[32] Gunawidjaja PN, Mathew R, Lo AYH, Izquierdo-Barba I, García A, Arcos D, et al. Local structures of mesoporous bioactive glasses and their surface alterations in vitro: inferences from solid-state nuclear magnetic resonance. 2012;370:1376-99.

[33] Oonishi H, Hench LL, Wilson J, Sugihara F, Tsuji E, Matsuura M, et al. Quantitative comparison of bone growth behavior in granules of Bioglass®, A-W glass-ceramic, and hydroxyapatite. J Biomed Mater Res 2000;51:37-46.

[34] Zhong J, Greenspan DC. Processing and properties of sol–gel bioactive glasses. J Biomed Mater Res 2000;53:694-701.

[35] Mastrogiacomo M, Muraglia A, Komlev V, Peyrin F, Rustichelli F, Crovace A, et al. Tissue engineering of bone: search for a better scaffold. Orthod Craniofac Res 2005;8:277-84.

[36] Elliott JC. Calcium Phosphate Biominerals. Rev Mineral Geochem 2002;48:427-53.

[37] Hughes JM, Rakovan J. The Crystal Structure of Apatite, Ca5(PO4)3(F,OH,Cl). Rev Mineral Geochem 2002;48:1-12.

[38] Thian ES, Huang J, Best SM, Barber ZH, Bonfield W. Novel silicon-doped hydroxyapatite (Si-HA) for biomedical coatings: An in vitro study using acellular simulated body fluid. J Biomed Mater Res B Appl Biomater 2006;76B:326-33.

[39] Sayer M, Stratilatov AD, Reid J, Calderin L, Stott MJ, Yin X, et al. Structure and composition of silicon-stabilized tricalcium phosphate. Biomaterials 2003;24:369-82.

[40] Gibson IR, Best SM, Bonfield W. Chemical characterization of silicon-substituted hydroxyapatite. J Biomed Mater Res 1999;44:422-8.

[41] Qiu ZY, Li G, Zhang YQ, Liu J, Hu W, Ma J, et al. Fine structure analysis and sintering properties of Si-doped hydroxyapatite. Biomed Mater 2012;7:045009.

[42] Gibson IR, Best SM, Bonfield W. Effect of Silicon Substitution on the Sintering and Microstructure of Hydroxyapatite. J Am Ceram Soc 2002;85:2771-7.

[43] Vallet-Regi M, Arcos D. Silicon substituted hydroxyapatites. A method to upgrade calcium phosphate based implants. J Mater Chem 2005;15:1509.

[44] Keeting PE, Oursler MJ, Wiegand KE, Bonde SK, Spelsberg TC, Riggs BL. Zeolite a increases proliferation, differentiation, and transforming growth factor β production in normal adult human osteoblast-like cells in vitro. J Bone Miner Res 1992;7:1281-9.

[45] Patel N, Best SM, Bonfield W, Gibson IR, Hing KA, Damien E, et al. A comparative study on the in vivo behavior of hydroxyapatite and silicon substituted hydroxyapatite granules. J Mater Sci: Mater Med 2002;13:1199-206.

[46] Porter AE, Patel N, Skepper JN, Best SM, Bonfield W. Effect of sintered silicate-substituted hydroxyapatite on remodelling processes at the bone–implant interface. Biomaterials 2004;25:3303-14.

[47] Porter AE, Patel N, Skepper JN, Best SM, Bonfield W. Comparison of in vivo dissolution processes in hydroxyapatite and silicon-substituted hydroxyapatite bioceramics. Biomaterials 2003;24:4609-20.

[48] Porter AE, Best SM, Bonfield W. Ultrastructural comparison of hydroxyapatite and silicon-substituted hydroxyapatite for biomedical applications. J Biomed Mater Res, Part A 2004;68A:133-41.

[49] Porter AE, Botelho CM, Lopes MA, Santos JD, Best SM, Bonfield W. Ultrastructural comparison of dissolution and apatite precipitation on hydroxyapatite and silicon-substituted hydroxyapatite in vitro and in vivo. J Biomed Mater Res, Part A 2004;69A:670-9.

[50] Botelho CM, Lopes MA, Gibson IR, Best SM, Santos JD. Structural analysis of Si-substituted hydroxyapatite: zeta potential and X-ray photoelectron spectroscopy. J Mater Sci: Mater Med 2002;13:1123-7.

[51] Cao H, Kuboyama N. A biodegradable porous composite scaffold of PGA/β-TCP for bone tissue engineering. Bone 2010;46:386-95.

[52] Pietak AM, Reid JW, Stott MJ, Sayer M. Silicon substitution in the calcium phosphate bioceramics. Biomaterials 2007;28:4023-32.

[53] Mostafa N, Shaltout A, Radev L, Hassan H. In vitro surface biocompatibility of high-content silicon-substituted calcium phosphate ceramics. Cent Eur J Chem 2013;11:140-50.

[54] Camiré CL, Jegou Saint-Jean S, Mochales C, Nevsten P, Wang J-S, Lidgren L, et al. Material characterization and in vivo behavior of silicon substituted α-tricalcium phosphate cement. J Biomed Mater Res B Appl Biomater 2006;76B:424-31.

[55] Mastrogiacomo M, Corsi A, Francioso E, Di Comite M, Monetti F, Scaglione S, et al. Reconstruction of extensive long bone defects in sheep using resorbable bioceramics based on silicon stabilized tricalcium phosphate. Tissue Eng 2006;12:1261-73.

[56] Ohura K, Nakamura T, Yamamuro T, Ebisawa Y, Kokubo T, Kotoura Y, et al. Bioactivity of CaO·SiO2 glasses added with various ions. J Mater Sci: Mater Med 1992;3:95-100.

[57] De Aza PN, Guitian F, De Aza S, Valle FJ. Analytical control of wollastonite for biomedical applications by use of atomic absorption spectrometry and inductively coupled plasma atomic emission spectrometry. The Analyst 1998;123:681-5.

[58] De Aza PN, Luklinska ZB, Anseau MR, Guitian F, De Aza S. Transmission electron microscopy of the interface between bone and pseudowollastonite implant. J Microsc 2001;201:33-43.

[59] De Aza PN, Luklinska ZB, Anseau MR, Guitian F, De Aza S. Bioactivity of pseudowollastonite in human saliva. J Dent 1999;27:107-13.

[60] De Aza PN, Luklinska ZB, Anseau MR, Hector M, Guitián F, De Aza S. Reactivity of a wollastonite–tricalcium phosphate Bioeutectic® ceramic in human parotid saliva. Biomaterials 2000;21:1735-41.

[61] De Aza PN, Fernández-Pradas JM, Serra P. In vitro bioactivity of laser ablation pseudowollastonite coating. Biomaterials 2004;25:1983-90.

[62] De Aza PN, Guitián F, De Aza S. A new bioactive material which transforms in situ into hydroxyapatite. Acta Mater 1998;46:2541-9.

[63] De Aza PN, Guitián F, De Aza S. Bioeutectic: a new ceramic material for human bone replacement. Biomaterials 1997;18:1285-91.

[64] Sahai N, Anseau M. Cyclic silicate active site and stereochemical match for apatite nucleation on pseudowollastonite bioceramic–bone interfaces. Biomaterials 2005;26:5763-70.

[65] Sahai N, Tossell JA. Molecular Orbital Study of Apatite (Ca5(PO4)3OH) Nucleation at Silica Bioceramic Surfaces. J Phys Chem B 2000;104:4322-41.

[66] Casey WH, Westrich HR, Banfield JF, Ferruzzi G, Arnold GW. Leaching and reconstruction at the surfaces of dissolving chain-silicate minerals. Nature 1993;366:253-6.

[67] Zhang N, Molenda JA, Fournelle JH, Murphy WL, Sahai N. Effects of pseudowollastonite (CaSiO3) bioceramic on in vitro activity of human mesenchymal stem cells. Biomaterials 2010;31:7653-65.

[68] Zhang N, Molenda JA, Mankoci S, Zhou X, Murphy WL, Sahai N. Crystal structures of CaSiO3 polymorphs control growth and osteogenic differentiation of human mesenchymal stem cells on bioceramic surfaces. Biomaterials Science 2013;1:1101-10.

[69] Dufrane D, Delloye C, McKay IJ, De Aza PN, De Aza S, Schneider YJ, et al. Indirect cytotoxicity evaluation of pseudowollastonite. J Mater Sci: Mater Med 2003;14:33-8.

[70] Sarmento C, Luklinska ZB, Brown L, Anseau M, De Aza PN, De Aza S, et al. In vitro behavior of osteoblastic cells cultured in the presence of pseudowollastonite ceramic. J Biomed Mater Res A 2004;69A:351-8.

[71] De Aza PN, De Aza AH, De Aza S. Crystalline bioceramic materials. Bol Soc Esp Ceram V 2005;44:135-45.

[72] Best SM, Porter AE, Thian ES, Huang J. Bioceramics: Past, present and for the future. J Eur Ceram Soc 2008;28:1319-27.

[73] Karageorgiou V, Kaplan D. Porosity of 3D biomaterial scaffolds and osteogenesis. Biomaterials 2005;26:5474-91.

[74] Rezwan K, Chen QZ, Blaker JJ, Boccaccini AR. Biodegradable and bioactive porous polymer/inorganic composite scaffolds for bone tissue engineering. Biomaterials 2006;27:3413-31.

[75] De Aza P, Peña J, Luklinska Z, Meseguer-Olmo L. Bioeutectic® Ceramics for Biomedical Application Obtained by Laser Floating Zone Method. In vivo Evaluation. Materials 2014;7:2395-410.

[76] Li P, Ohtsuki C, Kokubo T, Nakanishi K, Soga N, Nakamura T, et al. Apatite Formation Induced by Silica Gel in a Simulated Body Fluid. J Am Ceram Soc 1992;75:2094-7.

[77] Izquierdo-Barba I, Ruiz-González L, Doadrio JC, González-Calbet JM, Vallet-Regí M. Tissue regeneration: A new property of mesoporous materials. Solid State Sci 2005;7:983-9.

[78] Vallet-Regi M, Ruiz-Gonzalez L, Izquierdo-Barba I, Gonzalez-Calbet JM. Revisiting silica based ordered mesoporous materials: medical applications. J Mater Chem 2006;16:26-31.

[79] Canham LT. Bioactive silicon structure fabrication through nanoetching techniques. Adv Mater 1995;7:1033-7.

[80] Hench L. Biomaterials. Science 1980;208:826-31.

[81] Muthusubramaniam L, Lowe R, Fissell W, Li L, Marchant R, Desai T, et al. Hemocompatibility of Silicon-Based Substrates for Biomedical Implant Applications. Ann Biomed Eng 2011;39:1296-305.

[82] Sun W, Puzas JE, Sheu TJ, Liu X, Fauchet PM. Nano- to Microscale Porous Silicon as a Cell Interface for Bone-Tissue Engineering. Adv Mater 2007;19:921-4.

[83] Bohner M. Silicon-substituted calcium phosphates – A critical view. Biomaterials 2009;30:6403-6.

[84] Hench LL, Polak JM, Xynos ID, Buttery LDK. Bioactive materials to control cell cycle. Mater Res Innovations 2000;3:313-23.

[85] Xynos ID, Hukkanen MVJ, Batten JJ, Buttery LD, Hench LL, Polak JM. Bioglass ®45S5 stimulates osteoblast turnover and enhances bone formation *in vitro*: implications and applications for bone tissue engineering. Calcif Tissue Int 2000;67:321-9.

[86] Xynos ID, Edgar AJ, Buttery LDK, Hench LL, Polak JM. Ionic Products of Bioactive Glass Dissolution Increase Proliferation of Human Osteoblasts and Induce Insulin-like Growth Factor II mRNA Expression and Protein Synthesis. Biochem Biophys Res Commun 2000;276:461-5.

[87] Xynos ID, Edgar AJ, Buttery LDK, Hench LL, Polak JM. Gene-expression profiling of human osteoblasts following treatment with the ionic products of Bioglass® 45S5 dissolution. J Biomed Mater Res 2001;55:151-7.

[88] Pietak A. The role of silicon in Si-TCP bioceramics: a material and biological characterization. Kingston: Queen's University 2004.

[89] Balas F, Pérez-Pariente J, Vallet-Regí M. In vitro bioactivity of silicon-substituted hydroxyapatites. J Biomed Mater Res A 2003;66A:364-75.

[90] Elliot MA, Edwards HM. Effect of dietary silicon on growth and skeletal development in chickens. J Nutr 1991;121:201-7.

[91] ELLIOT MA, EDWARDS HM. Some Effects of Dietary Aluminum and Silicon on Broiler Chickens. Poult Sci 1991;70:1390-402.

[92] Kayongo-Male H, Jia X. Silicon bioavailability studies in young rapidly growing rats and turkeys fed semipurified diets. Biol Trace Elem Res 1999;67:173-86.

[93] Seaborn C, Nielsen F. Effects of germanium and silicon on bone mineralization. Biol Trace Elem Res 1994;42:151-64.

[94] Seaborn C, Nielsen F. High dietary aluminum affects the response of rats to silicon deprivation. Biol Trace Elem Res 1994;41:295-304.

[95] Jugdaohsingh R, Calomme MR, Robinson K, Nielsen F, Anderson SHC, D'Haese P, et al. Increased longitudinal growth in rats on a silicon-depleted diet. Bone 2008;43:596-606.

[96] Reffitt DM, Ogston N, Jugdaohsingh R, Cheung HFJ, Evans BAJ, Thompson RPH, et al. Orthosilicic acid stimulates collagen type 1 synthesis and osteoblastic differentiation in human osteoblast-like cells in vitro. Bone 2003;32:127-35.

[97] Arumugam MQ, Ireland DC, Brooks RA, Rushton N, Bonfield W. Orthosilicic acid increases collagen type I mRNA expression in human bone-derived osteoblasts in vitro. In: Barbosa MA, Monteiro FJ, Correia R, Leon B, editors. Bioceramics, Vol 16. Zurich-Uetikon: Trans Tech Publications Ltd; 2004. p. 869-72.

[98] Arumugam MQ, Ireland DC, Brooks RA, Rushton N, Bonfield W. The effect orthosilicic acid on collagen type I, alkaline phosphatase and osteocalcin mRNA expression in human bone-derived osteoblasts in vitro. In: Nakamura T, Yamashita K, Neo M, editors. Bioceramics 18, Pts 1 and 2. Zurich-Uetikon: Trans Tech Publications Ltd; 2006. p. 121-4.

[99] Beertsen W, van den Bos T. Alkaline phosphatase induces the mineralization of sheets of collagen implanted subcutaneously in the rat. J Clin Invest 1992;89:1974-80.

[100] Nuttelman CR, Benoit DS, Tripodi MC, Anseth KS. The effect of ethylene glycol methacrylate phosphate in PEG hydrogels on mineralization and viability of encapsulated hMSCs. Biomaterials 2006;27:1377-86.

[101] Zou S, Ireland D, Brooks RA, Rushton N, Best S. The effects of silicate ions on human osteoblast adhesion, proliferation, and differentiation. J Biomed Mater Res B Appl Biomater 2009;90B:123-30.

[102] Mladenović Ž, Johansson A, Willman B, Shahabi K, Björn E, Ransjö M. Soluble silica inhibits osteoclast formation and bone resorption in vitro. Acta Biomater 2014;10:406-18.

[103] Beck Jr GR, Ha S-W, Camalier CE, Yamaguchi M, Li Y, Lee J-K, et al. Bioactive silica-based nanoparticles stimulate bone-forming osteoblasts, suppress bone-resorbing osteoclasts, and enhance bone mineral density in vivo. Nanomed Nanotechnol 2012;8:793-803.

[104] Gaharwar AK, Mihaila SM, Swami A, Patel A, Sant S, Reis RL, et al. Bioactive Silicate Nanoplatelets for Osteogenic Differentiation of Human Mesenchymal Stem Cells. Adv Mater 2013;25:3329-36.

[105] Ha S-W, Weitzmann MN, Beck GR. Bioactive Silica Nanoparticles Promote Osteoblast Differentiation through Stimulation of Autophagy and Direct Association with LC3 and p62. ACS Nano 2014;8:5898-910.

[106] Huang D-M, Hung Y, Ko B-S, Hsu S-C, Chen W-H, Chien C-L, et al. Highly efficient cellular labeling of mesoporous nanoparticles in human mesenchymal stem cells: implication for stem cell tracking. FASEB J 2005;19:2014-6.

[107] Wiens M, Wang X, Schröder HC, Kolb U, Schloßmacher U, Ushijima H, et al. The role of biosilica in the osteoprotegerin/RANKL ratio in human osteoblast-like cells. Biomaterials 2010;31:7716-25.

[108] Zhou X, Moussa FM, Mankoci S, Ustriyana P, Zhang N, Abdelmagid S, et al. Orthosilicic acid, Si(OH)4, stimulates osteoblast differentiation in vitro by upregulating miR-146a to antagonize NF-κB activation. Acta Biomater 2016;39:192-202.

[109] Iler RK. The chemistry of silica: solubility, polymerization, colloid and surface properties, and biochemistry. 1979.

FIGURE CAPTIONS

Figure 1. Beneficial effect of silicate on bone is illustrated by these four-week old chickens. The chicken to the left was fed a diet with high levels of silicate (100 mg/g) while the one to the right was fed a diet with low levels of silicate (2 mg/g). (Photo: Carlisle, 1972)

Figure 2. Bioactive regions in the CaO-SiO_2-Na_2O system. All glasses contain 6% wt of P_2O_5. Glasses and glass-ceramics that have a composition falling inside region A develop HAP both *in vitro* and *in vivo*. Compositions inside the dashed line also bond to soft tissues. The compositions in region B such as window and bottle glass are inert and a fibrous capsule is formed around them when implanted; those in region C are completely dissolved at 10-30 days following implantation. Region D is a non-glass forming and non-bonding region. Glasses within region E (dashed curves) adhere to collagen, the soft tissue component of bone. Reproduced with permission [29]. Copyright 2005, John Wiley & Sons, Inc.

Figure 3. Schematic illustration of the reaction sequence leading to HCA formation according to Hench and co-workers, from a bioactive melt-prepared CaO-SiO_2 glass. Reproduced with permission [37]. Copyright 2012, The Royal Society.

Figure 4. Schematic diagram of the lattices of pure HA and Si-HA. Silicate anions (SiO_4^{4-}) substitute phosphate anion (PO_4^{3-}) in the apatite crystal lattice albeit to a limited extent. Reproduced with permission [41]. Copyright 2012, IOP Publishing Ltd.

Figure 5. Gross cross section (top panels) and contact microradiographs (bottom panels) of Si-α-TCP scaffolds implanted in the tibiae of sheep sacrificed at 3, 6 and 24 months after surgery. At 3 months, the cross-sectional shape of the implant is still recognizable and the newly-formed bone is mainly deposited on its external surface. At 6 months, the loss of the central canal of the

hollow implant occurs as a result of both implant fragmentation and new bone formation within the inner pores. At 24 months, the implant phase is markedly reduced, and very few and sparse fragments can be detected (arrows). Scale bar shows 5 mm. Reproduced with permission [55]. Copyright 2006, Mary Ann Liebert, Inc.

Figure 6. Schematic of the crystal structure of β-$CaSiO_3$ and α-$CaSiO_3$. Legend for atoms in panels: O = red, Si = blue, Ca = green.

Figure 7. Schematic representation of the first stages (a) and final stage (b) of HAP formation in eutectic material after immersion in SBF. Reproduced with permission [63] with slight modification. Copyright 1997, published by Elsevier Ltd.

Figure 8. SEM micrographs and EDS spectra of SBA-15, MCM-48 and MCM-41 materials at 0, 15, 30 and 60 d. Reproduced with permission [77]. Copyright 2006, The Royal Society.

Figure 9. Schematic representing the intrinsic biological effects of silica-based nanoparticles on osteoblast differentiation. Nanoparticles are internalized by caveolae-mediated endocytosis, which triggers a signal transduction pathway dependent on ERK1/2. This stimulation of ERK1/2 is necessary for the processing of LC3β form I to the activated form II. Nanoparticles are bound by both LC3 and p62, resulting in the formation of autophagosomes. The stimulation of autophagy is necessary for osteoblast differentiation and mineralization. Reproduced with permission [105]. Copyright 2014, published by American Chemical Society.

Figure 10. Proposed effects of biosilica on osteoblasts, osteoclasts, and their progenitors. Biosilica enhances expression of OPG in osteoblasts. Osteoblasts have the potential to differentiate to osteocytes and lining cells. OPG counteracts various effects of RANKL, a

cytokine that induces pre-osteoclast maturation and osteoclast activation. Reproduced with permission [106]. Copyright 2014, published by Elsevier Ltd.

Figure 11. $Si(OH)_4$-mediated regulation of NF-κB via miR-146a in bone cells. $Si(OH)_4$ may enter the cell through Na+-HCO_3^- co-transporter (NBC-1). Within the cell $Si(OH)_4$ can induce the expression of endogenous miR-146a to reduce activation of NF-κB. The inhibition of NF-κB results in activation of Runx2, the master transcription factor necessary for osteoblast precursor differentiation. This deactivation of NF-κB also inhibits the expression of NFATc1, the key transcription gene for osteoclast precursor differentiation. Thus, $Si(OH)_4$ can stimulate osteoblast differentiation and inhibit osteoclast differentiation by antagonizing NF-κB activation via miR-146a, which implies a potential role in bone remodeling. Reproduced with permission [108]. Copyright 2016, published by Elsevier Ltd.

Table 1. Families of genes in primary human osteoblasts activated or up-regulated by ionic dissolution products of bioactive glasses. Reproduced with permission [2]. Copyright 2008 published by Elsevier Ltd.

Transcription factors and cell cycle regulators	**Activation (%)**
RCL growth-related c-myc-responsive gene	500
G1/S-specific cyclin D1 (CCND1)	400
26S proteinase regulatory subunit 6A	400
Cyclin-dependent kinase inhibitor 1 (CDKN1A)	350
cAMP-dependent transcription factor ATF-4	240
Cyclin K	200
DNA synthesis, repair and recombination	**Up-regulation (%)**
DNA exclusion repair protein ERCC	300
mutL protein homolog	300
High-mobility-group protein (HMG-1)	230
Replication factor C 38 kDa subunit (RFC38)	200
Apoptosis regulators	**Up-regulation (%)**
Defender against cell death 1 (DAD-1)	450
Ca-dependent proteinase small (regulatory) subunit; calpain	410
Deoxyribonuclease II (Dnase II)	160
Growth factors and cytokines	**Activation (%)**
Insulin-like growth factor II (IGF-II)	300

36

Macrophage-specific colony stimulating factor (CSF1; MCSF)	260
Bone-derived growth factor	200
Vascular endothelial growth factor precursor (VEGF)	200

Cell surface antigens and receptors	**Activation (%)**
CD44 antigen hematopoetic form precursor	700
Fibronectin receptor beta subunit; integrin beta 1	600
N-sam; fibroblast growth factor receptor-1 precursor	300
Vascular cell adhesion protein-1 precursor (V-CAM1)	200

Signal transduction molecules	**Activation (%)**
MAP kinase-activated protein kinase 2 (MAPKAP kinase 2)	600
Dual specificity nitrogen-activated protein kinase 2	200
ADP-ribosylation factor 1	200

Extracellular matrix compounds	**Activation (%)**
Matrix metalloproteinase 14 precursor (MMP 14)	370
Matrix metalloproteinase 2 (MMP 2)	270
Metalloproteinase 1 inhibitor precursor (TIMP 1)	220
TIMP 2 (MI)	220
Bone proteoglycan II precursor; decorin	200

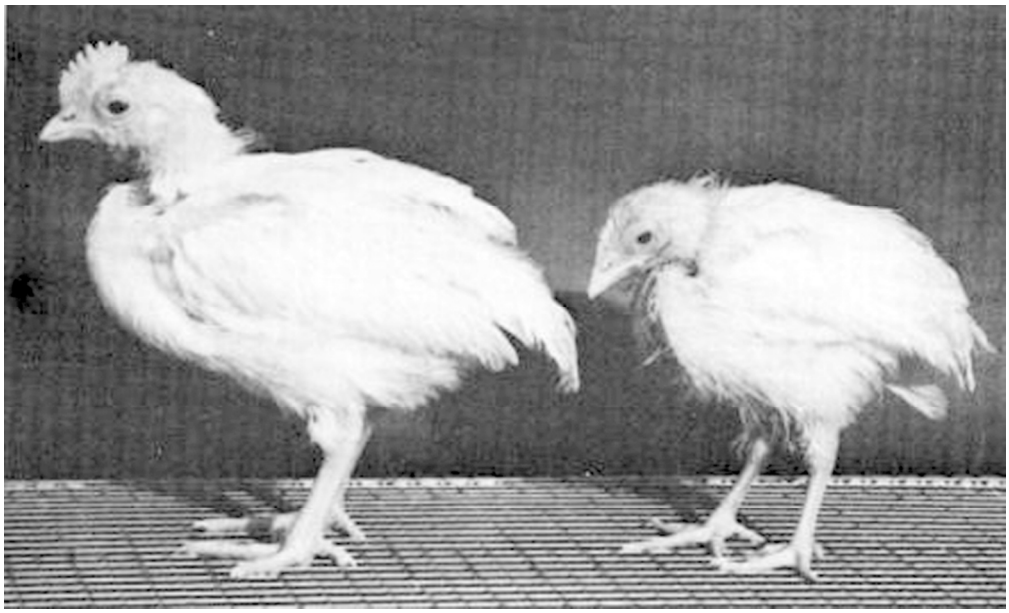

Figure 1. Beneficial effect of silicate on bone is illustrated by these four-week old chickens. The chicken to the left was fed a diet with high levels of silicate (100 mg/g) while the one to the right was fed a diet with low levels of silicate (2 mg/g). (Photo: Carlisle, 1972)

80x48mm (300 x 300 DPI)

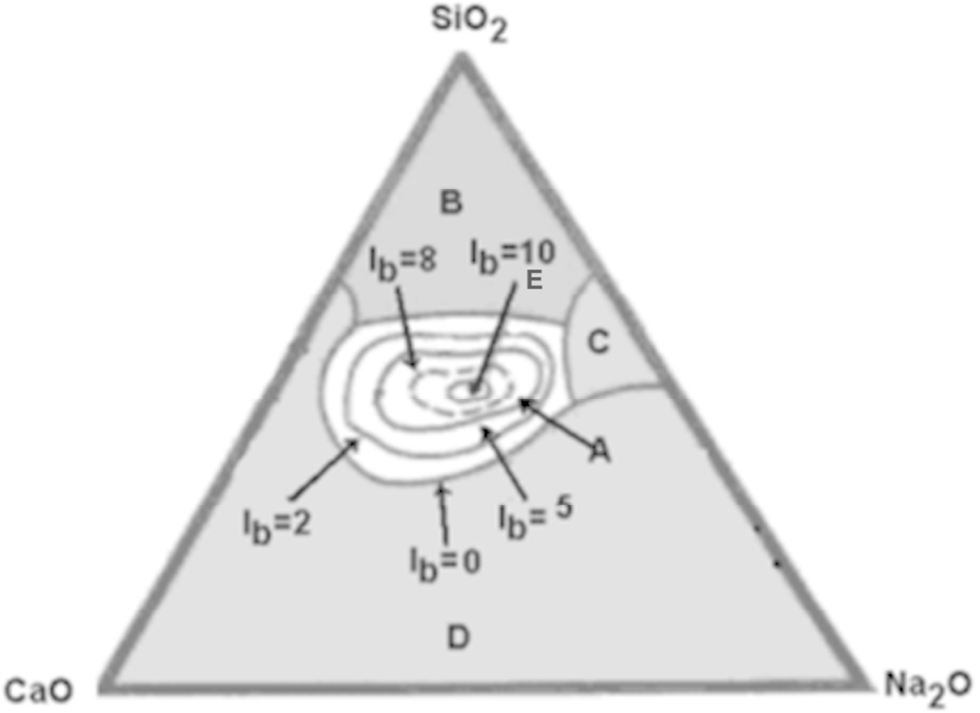

Figure 2. Bioactive regions in the CaO-SiO2-Na2O system. All glasses contain 6% wt of P2O5. Glasses and glass-ceramics that have a composition falling inside region A develop HAP both in vitro and in vivo. Compositions inside the dashed line also bond to soft tissues. The compositions in region B such as window and bottle glass are inert and a fibrous capsule is formed around them when implanted; those in region C are completely dissolved at 10-30 days following implantation. Region D is a non-glass forming and non-bonding region. Glasses within region E (dashed curves) adhere to collagen, the soft tissue component of bone. Reproduced with permission [29]. Copyright 2005, John Wiley & Sons, Inc.

80x58mm (300 x 300 DPI)

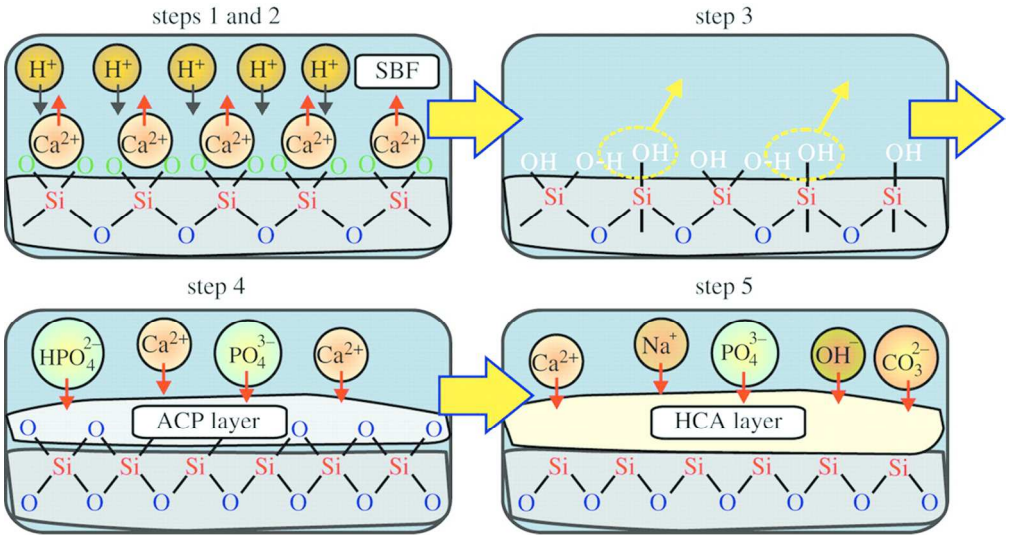

Figure 3. Schematic illustration of the reaction sequence leading to HCA formation according to Hench and co-workers, from a bioactive melt-prepared CaO-SiO2 glass. Reproduced with permission [37]. Copyright 2012, The Royal Society.

119x63mm (300 x 300 DPI)

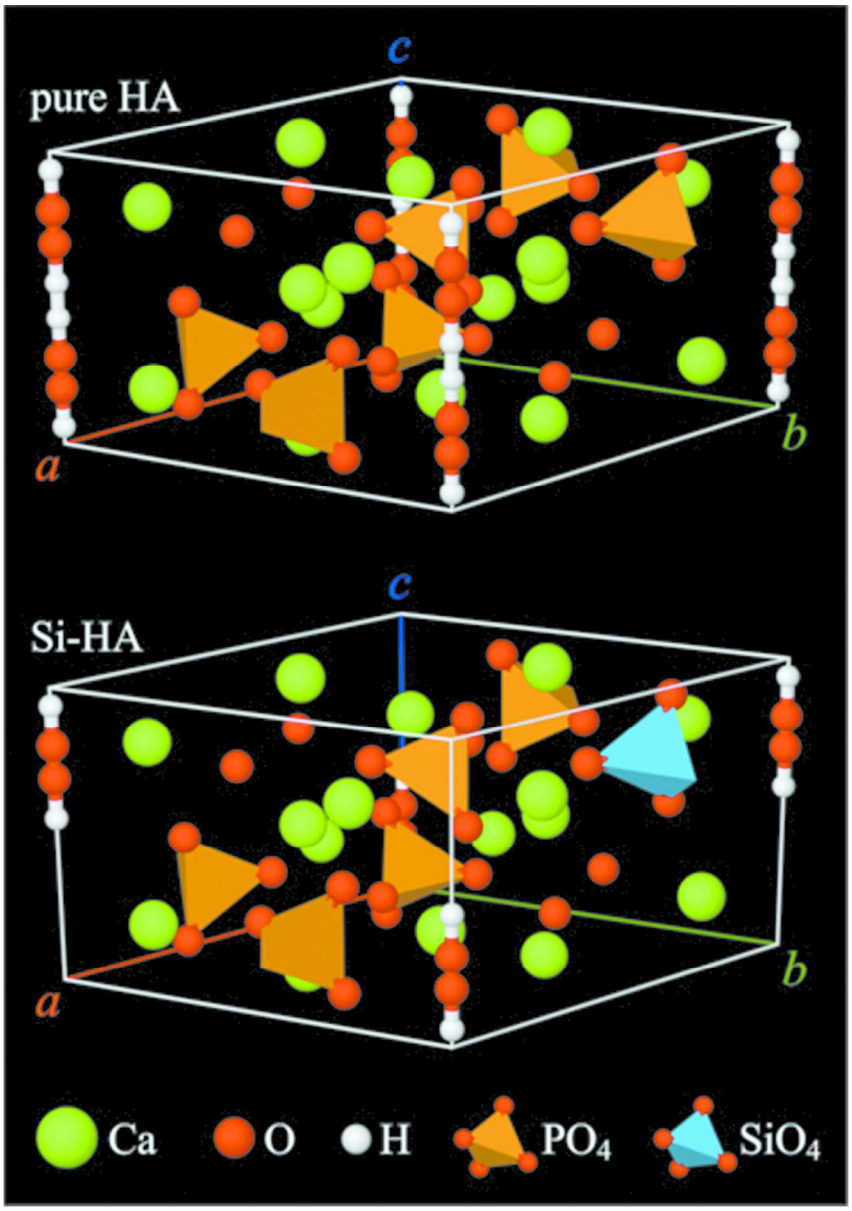

Figure 4. Schematic diagram of the lattices of pure HA and Si-HA. Silicate anions (SiO44-) substitute phosphate anion (PO43-) in the apatite crystal lattice albeit to a limited extent. Reproduced with permission [41]. Copyright 2012, IOP Publishing Ltd.

60x85mm (300 x 300 DPI)

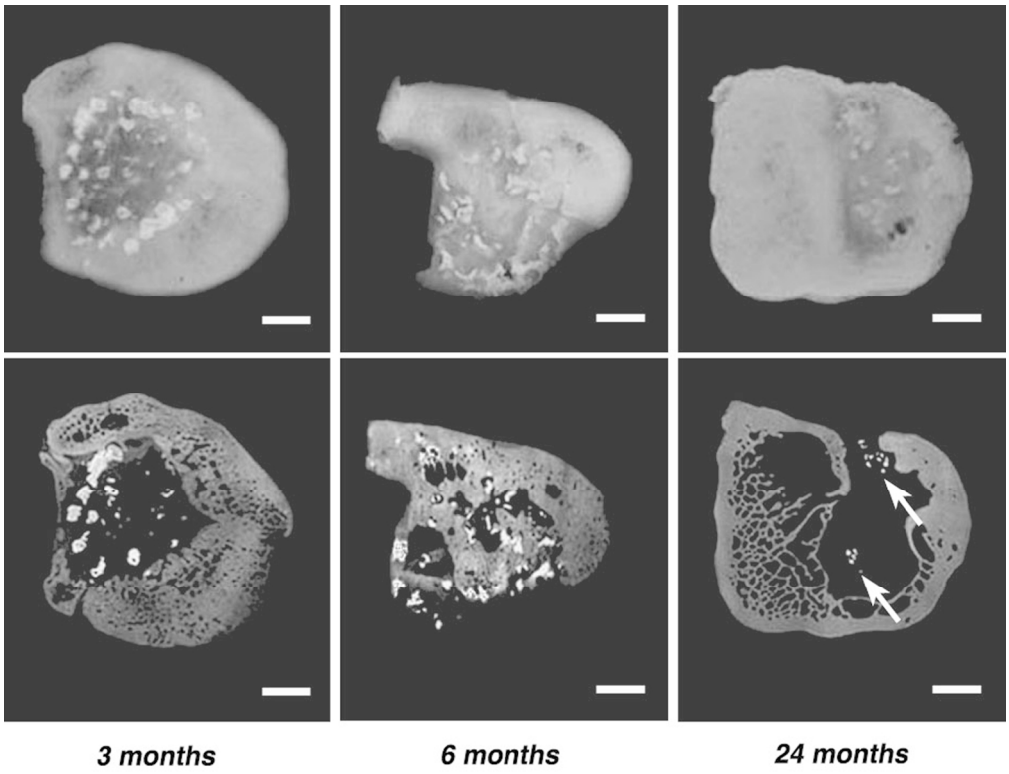

Figure 5. Gross cross section (top panels) and contact microradiographs (bottom panels) of Si-α- TCP scaffolds implanted in the tibiae of sheep sacrificed at 3, 6 and 24 months after surgery. At 3 months, the cross-sectional shape of the implant is still recognizable and the newly-formed bone is mainly deposited on its external surface. At 6 months, the loss of the central canal of the hollow implant occurs as a result of both implant fragmentation and new bone formation within the inner pores. At 24 months, the implant phase is markedly reduced, and very few and sparse fragments can be detected (arrows). Scale bar shows 5 mm. Reproduced with permission [55]. Copyright 2006, Mary Ann Liebert, Inc.

140x108mm (300 x 300 DPI)

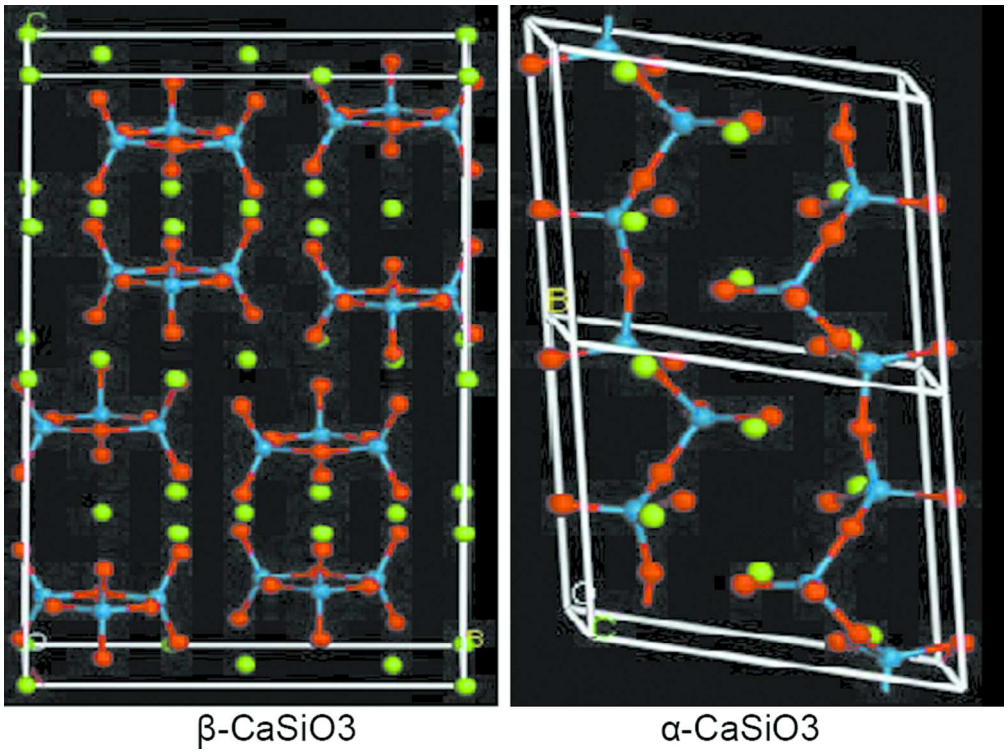

Figure 6. Schematic of the crystal structure of β-CaSiO3 and α-CaSiO3. Legend for atoms in panels: O = red, Si = blue, Ca = green.

80x59mm (300 x 300 DPI)

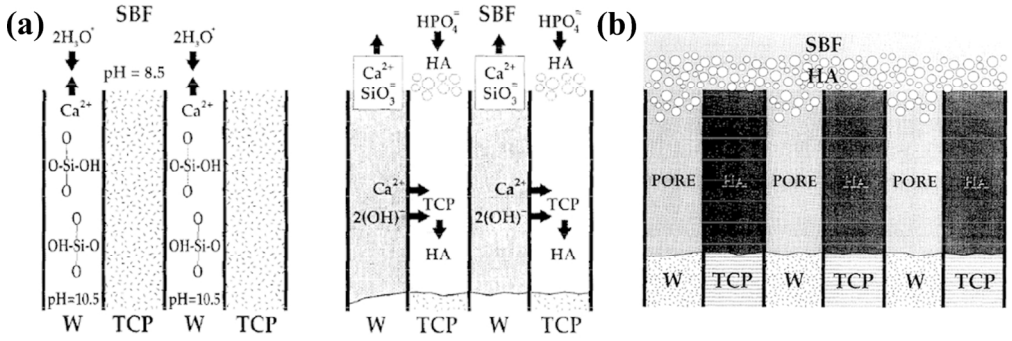

Figure 7. Schematic representation of the first stages (a) and final stage (b) of HAP formation in eutectic material after immersion in SBF. Reproduced with permission [63] with slight modification. Copyright 1997, published by Elsevier Ltd.

150x50mm (300 x 300 DPI)

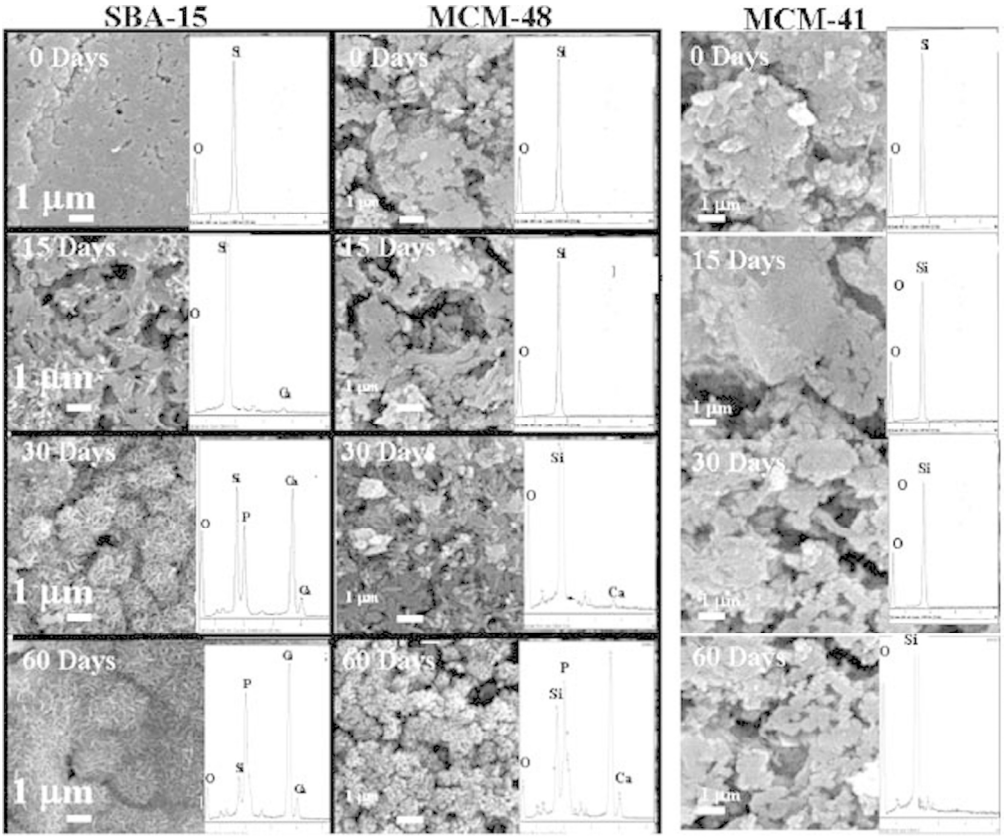

Figure 8. SEM micrographs and EDS spectra of SBA-15, MCM-48 and MCM-41 materials at 0, 15, 30 and 60 d. Reproduced with permission [77]. Copyright 2006, The Royal Society.

140x117mm (300 x 300 DPI)

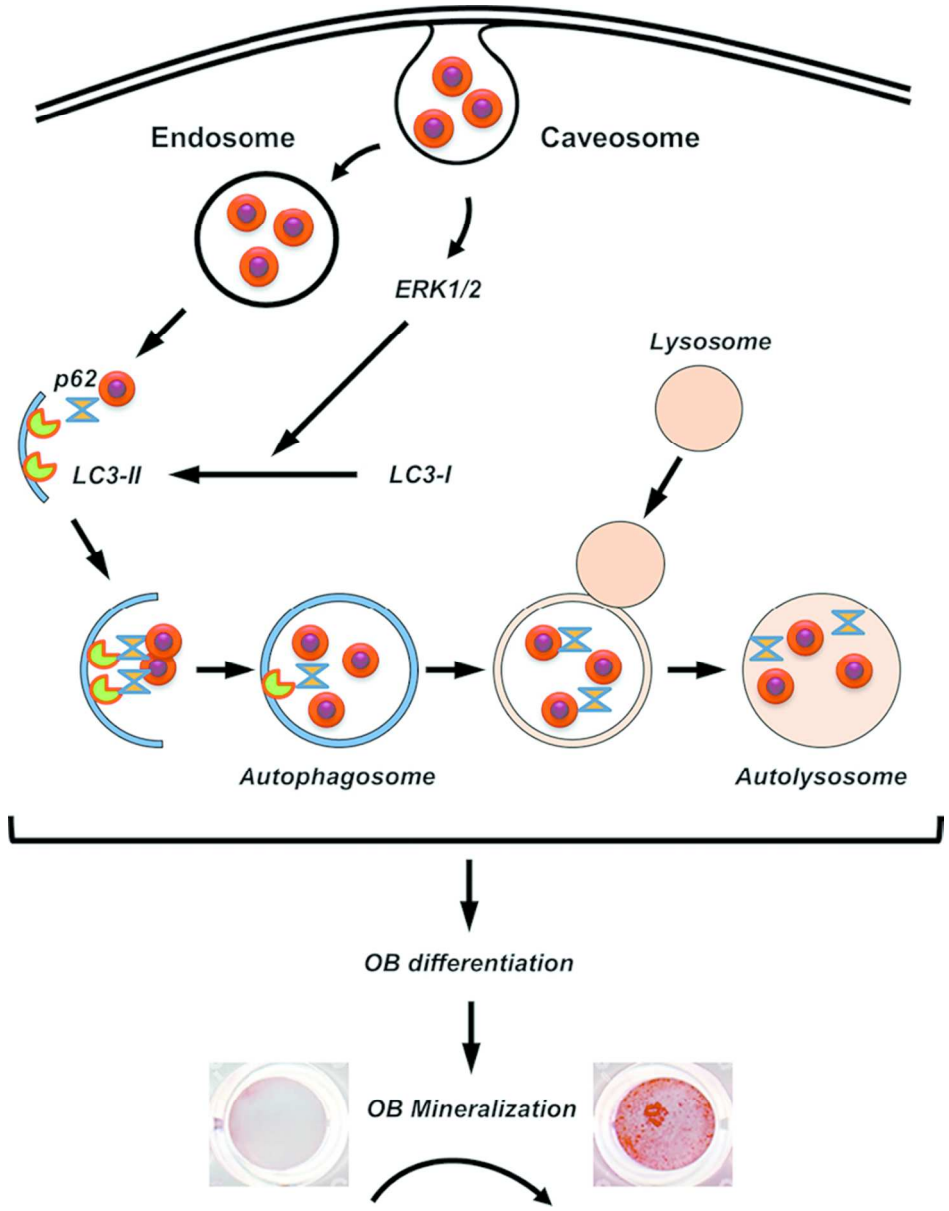

Figure 9. Schematic representing the intrinsic biological effects of silica-based nanoparticles on osteoblast differentiation. Nanoparticles are internalized by caveolae-mediated endocytosis, which triggers a signal transduction pathway dependent on ERK1/2. This stimulation of ERK1/2 is necessary for the processing of LC3β form I to the activated form II. Nanoparticles are bound by both LC3 and p62, resulting in the formation of autophagosomes. The stimulation of autophagy is necessary for osteoblast differentiation and mineralization. Reproduced with permission [105]. Copyright 2014, published by American Chemical Society.

80x102mm (300 x 300 DPI)

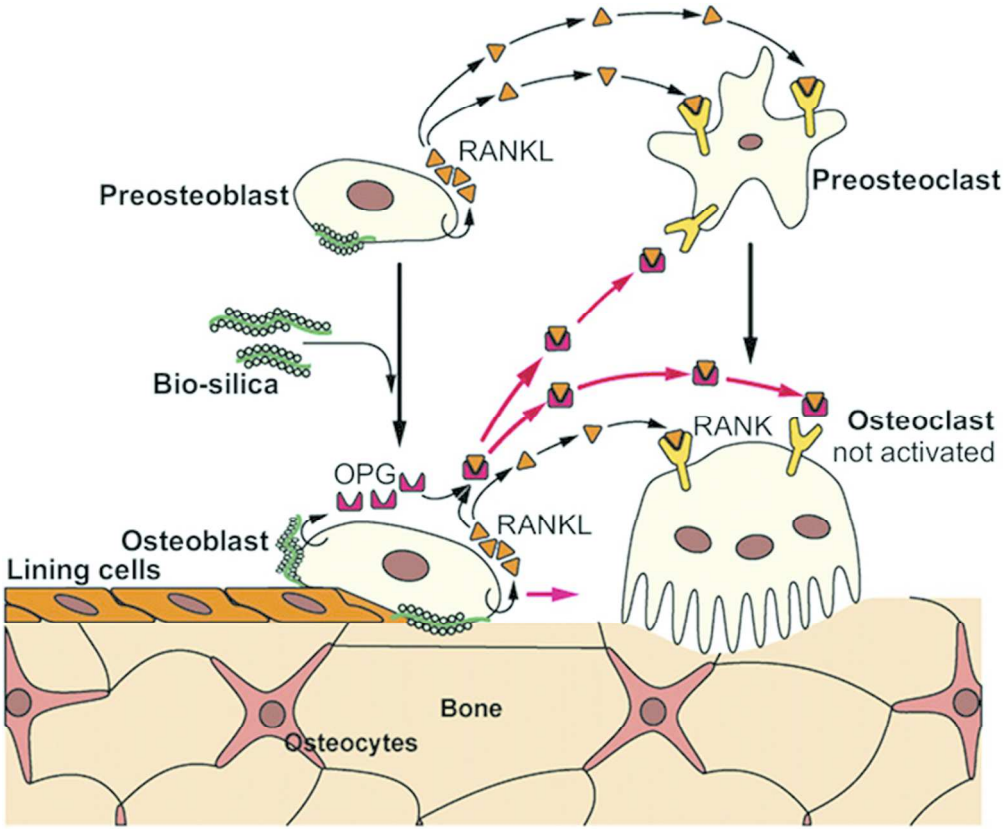

Figure 10. Proposed effects of biosilica on osteoblasts, osteoclasts, and their progenitors. Biosilica enhances expression of OPG in osteoblasts. Osteoblasts have the potential to differentiate to osteocytes and lining cells. OPG counteracts various effects of RANKL, a cytokine that induces pre-osteoclast maturation and osteoclast activation. Reproduced with permission [106]. Copyright 2014, published by Elsevier Ltd.

80x65mm (300 x 300 DPI)

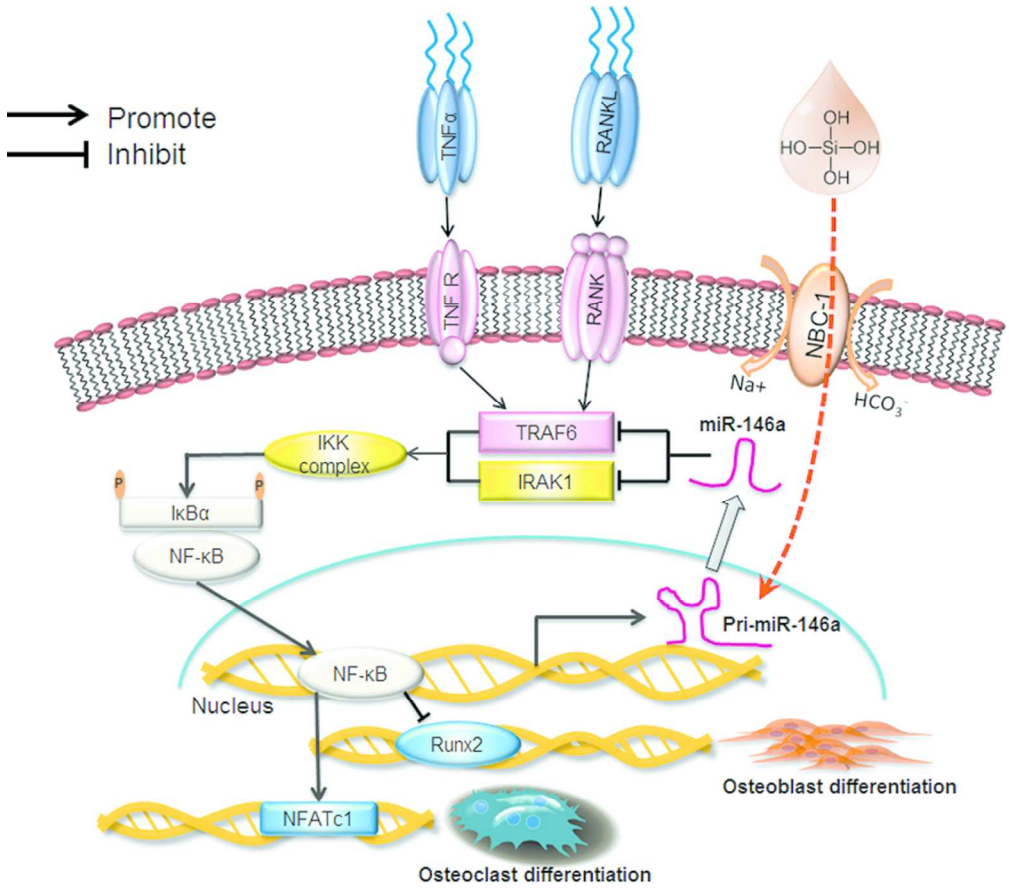

Figure 11. Si(OH)4-mediated regulation of NF-κB via miR-146a in bone cells. Si(OH)4 may enter the cell through Na+-HCO3- co-transporter (NBC-1). Within the cell Si(OH)4 can induce the expression of endogenous miR-146a to reduce activation of NF-κB. The inhibition of NF-κB results in activation of Runx2, the master transcription factor necessary for osteoblast precursor differentiation. This deactivation of NF-κB also inhibits the expression of NFATc1, the key transcription gene for osteoclast precursor differentiation. Thus, Si(OH)4 can stimulate osteoblast differentiation and inhibit osteoclast differentiation by antagonizing NF-κB activation via miR-146a, which implies a potential role in bone remodeling. Reproduced with permission [108]. Copyright 2016, published by Elsevier Ltd.

99x88mm (300 x 300 DPI)